

Inelastic x-ray scattering measurements of phonon dispersion and lifetimes in $\text{PbTe}_{1-x}\text{Se}_x$ alloys

Zhiting Tian¹, Mingda Li², Zhensong Ren³, Hao Ma¹, Ahmet Alatas⁴, Stephen D Wilson⁵ and Ju Li²

¹ Department of Mechanical Engineering, Virginia Tech, Blacksburg, Virginia 24061, USA

² Department of Nuclear Science and Engineering, Massachusetts Institute of Technology, Cambridge, Massachusetts 02139, USA

³ Department of Physics, Boston College, Chestnut Hill, Massachusetts 02467, USA

⁴ Advanced Photon Source, Argonne National Laboratory, Argonne, Illinois 64039, USA

⁵ Department of Materials, University of California, Santa Barbara, Santa Barbara, 93106, USA

E-mail: zhiting@vt.edu and mingda@mit.edu

Received 12 June 2015, revised 25 July 2015

Accepted for publication 10 August 2015

Published 2 September 2015



CrossMark

Abstract

$\text{PbTe}_{1-x}\text{Se}_x$ alloys are of special interest to thermoelectric applications. Inelastic x-ray scattering determination of phonon dispersion and lifetimes along the high symmetry directions for $\text{PbTe}_{1-x}\text{Se}_x$ alloys are presented. By comparing with calculated results based on the virtual crystal model calculations combined with *ab initio* density functional theory, the validity of virtual crystal model is evaluated. The results indicate that the virtual crystal model is overall a good assumption for phonon frequencies and group velocities despite the softening of transverse acoustic phonon modes along [1 1 1] direction, while the treatment of lifetimes warrants caution. In addition, phonons remain a good description of vibrational modes in $\text{PbTe}_{1-x}\text{Se}_x$ alloys.

Keywords: thermoelectric, inelastic x-ray scattering, alloy

(Some figures may appear in colour only in the online journal)

Thermoelectric energy conversion, a direct conversion from thermal into electrical energy, has attracted intensive attention due to its potential to harness waste heat and contribute to globally applicable renewable energy solutions [1–7]. The efficiency of thermoelectric energy conversion is characterized by the dimensionless figure-of-merit ZT , defined as $ZT = S^2\sigma T/k$ where S , σ , k , T represent the Seebeck coefficient, electrical conductivity, thermal conductivity and absolute temperature, respectively. To improve ZT , low thermal conductivity is desired to maintain a large temperature gradient while reducing heat loss. Alloying is one traditional and proven way to reduce the lattice thermal conductivity without much degradation to electrical conductivity. Most of the state-of-art high ZT materials involve alloying [1–7], and $\text{PbTe}_{1-x}\text{Se}_x$ alloys are promising thermoelectric materials in the intermediate temperature range (600–800 K) [2, 3, 8].

While pure PbSe and PbTe have shown thermal conductivity as low as $\sim 2 \text{ W mK}^{-1}$, the thermal conductivity can be further reduced by alloying [9]. As a result, $\text{PbTe}_{1-x}\text{Se}_x$ alloys were reported to have ZT as high as 1.6–1.8 [8, 10]. Building from this, a thorough understanding of thermal transport in alloys will facilitate continued material design to further reduce the thermal conductivity for thermoelectric and other applications such as thermal insulation.

In dielectrics and semiconductors, heat is primarily carried by lattice vibration [11]. In perfect crystalline structures with well-defined periodicity, lattice vibrations can be well described by phonons. In the presence of substantial disorder, whether phonons remain a good description of crystal dynamics is controversial because the pure plane-wave description may become ill-defined. One goal of this work is to evaluate whether the vibrational modes can still

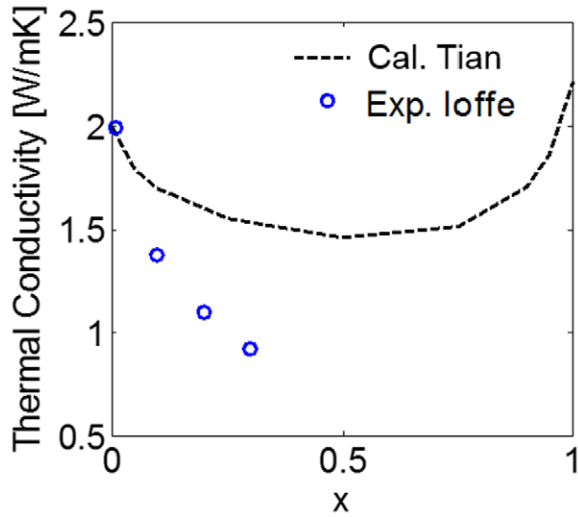


Figure 1. Thermal conductivity as a function of composition for $\text{PbTe}_{1-x}\text{Se}_x$ alloys by VC calculation [9] and experimental measurements [20].

be well represented by phonons in $\text{PbTe}_{1-x}\text{Se}_x$ alloys despite the potential existence of diffusons [12–14]. We first assume phonons are applicable and then check the validity at the end.

Theoretical study of vibrational modes in alloy systems is limited due to the breaking of the long-range translational symmetry. One typical approach to estimate the vibrational modes' behaviors is the virtual crystal (VC) model [15], where the disordered crystal is replaced with an ordered one of the average lattice parameter, atomic mass and force constants according to the composition. Both phonon–phonon and phonon-disorder scattering are included as perturbations [9, 14–17]. Using force constants from *ab initio* density functional perturbation theory (DFPT) calculations and taking into account mass disorder, the VC model was able to well reproduce the experimental thermal conductivity of $\text{Si}_{1-x}\text{Ge}_x$ alloys [17]. Applying the same approach to $\text{PbTe}_{1-x}\text{Se}_x$ alloys, the calculated results, however, significantly underestimate the alloy induced reduction in thermal conductivity as shown in figure 1. This calls into question the applicability of the VC model. For instance, it is questionable to only include first-order perturbation instead of full-order perturbation for scattering rates once the VC model departs from the dilute limit (x is close to 0 or 1). It is unclear how the scattering picture transitions from isolated scatterers in the dilute limit to dependent scattering in the non-dilute mixing limit (x is close to 0.5), which is similar to localized and extended states in electronic materials. Meanwhile, whether the independent scattering theory overestimates or underestimates the scattering rates strongly depends on the frequency range and the system itself because the wave interference may result in phonon localization or weaker phonon-disorder scattering [14, 18, 19]. It is also reasonable to question why the perturbation theory should hold at all in the non-dilute limit. Additionally, there are general open questions about alloys. For example, if one uses a supercell to calculate alloys, the group velocities diminish due to zone folding. The proper treatment of phonon group velocities has been under debate.

Table 1. The targeted sample compositions and measured mean atomic percent from EDX measurements.

Targeted composition	Measured mean atomic percent (%)		
	Pb	Te	Se
$\text{PbTe}_{0.25}\text{Se}_{0.75}$	50.24 ± 0.67	11.51 ± 0.21	38.25 ± 0.50
$\text{PbTe}_{0.5}\text{Se}_{0.5}$	50.53 ± 0.18	26.21 ± 0.10	23.26 ± 0.08

On the other hand, experimental data are limited for $\text{PbTe}_{1-x}\text{Se}_x$ alloys, making it difficult to assess the validity of the VC model. In this work, we report measurements of the phonon dispersion and linewidths of $\text{PbTe}_{1-x}\text{Se}_x$ alloys using high-energy resolution inelastic x-ray scattering (IXS). The main purpose of this work is to close the gap between the experimental data and theoretical data, and offer insights on those open questions in thermal transport of alloys. By comparing the experimental data with calculated values based on the VC model, we mainly discuss the validity of VC model and address fundamental questions about mode description in alloys.

Thermal conductivity, k , based on the Boltzmann equation under the relaxation time approximation is given by the well-known formula [21]

$$k = \frac{1}{3\Omega N_0} \sum_{qs} v_{qs}^2 \tau_{qs} \hbar \omega_{qs} \frac{\partial n_{qs}}{\partial T} \quad (1)$$

where Ω is the volume of the unit cell, v is the amplitude of group velocity, τ is the lifetime, ω is the frequency and n is the Bose–Einstein distribution. For a given material, frequency, group velocity and lifetime are the three key parameters to determine thermal conductivity. Lifetimes are reciprocal to the linewidths of phonon peaks.

Single crystals of $\text{PbTe}_{1-x}\text{Se}_x$ alloys were grown by an unseeded physical vapor transport method [22]. The starting materials of Pb, Te, and Se of purity 99.999% from Alfa Aesar were loaded into a quartz ampoule with a diameter of 0.5 in. in an Ar environment. The ampoule was evacuated to about 3×10^{-6} mbar, then quickly sealed using a hydrogen torch and loaded into a box furnace. The ampoule was heated up to 1075 °C, soaked for 5 h, and then furnace quenched down to room temperature. The broken pieces of the precursor were sealed and uniformly distributed horizontally in an evacuated quartz ampoule. The ampoule was then placed in a horizontal tube furnace and one end of the furnace was held at 850 °C for 4 d followed by slow cooling at a rate of about 50 °C h⁻¹ down to room temperature. This allowed crystals to nucleate and grow at the cooler end of the ampoule. Square-shaped and plate-like crystals up to a few millimeters in size were obtained and the Θ – 2Θ scan data from a Bruker D2 Phaser system determined the crystal facet to be (1 0 0) for all the stoichiometry ratios. The single crystals were then thinned down to the thicknesses of ~20–25 μm by a combination of focused ion beam and mechanical thinning.

We prepared two samples: $\text{PbTe}_{0.25}\text{Se}_{0.75}$, and $\text{PbTe}_{0.5}\text{Se}_{0.5}$. The chemical composition of each crystal has been determined by energy dispersive x-ray spectroscopy (EDX). Table 1 summarizes the EDX results. The actual compositions are fairly close to the targeted ones.

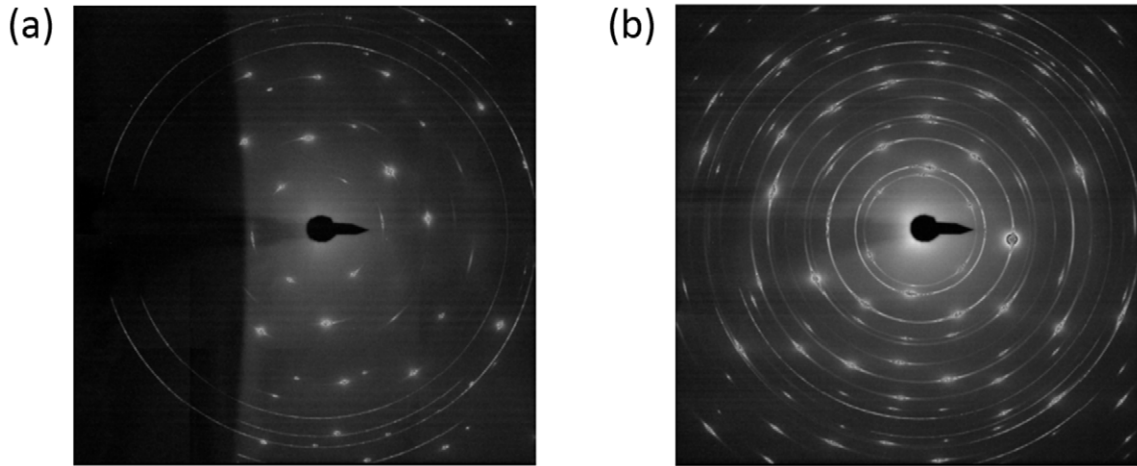


Figure 2. XRD patterns of (a) $\text{PbTe}_{0.25}\text{Se}_{0.75}$ and (b) $\text{PbTe}_{0.5}\text{Se}_{0.5}$.

Based on the x-ray diffraction (XRD) as shown in figure 2, both samples demonstrate single-crystalline features. The lattice constants of $\text{PbTe}_{0.25}\text{Se}_{0.75}$ and $\text{PbTe}_{0.5}\text{Se}_{0.5}$ were found to be 6.221 Å and 6.311 Å, respectively. The full width at half maximum (FWHM) of rocking curve of $\text{PbTe}_{0.25}\text{Se}_{0.75}$ measured at [220] reflection is 0.12° . Most of the Bragg reflections on XRD patterns of $\text{PbTe}_{0.5}\text{Se}_{0.5}$ were elongated transversely to short lines, though. This indicates that the structures of $\text{PbTe}_{0.5}\text{Se}_{0.5}$ slightly deviate from those of perfect crystals.

The inelastic x-ray scattering (IXS) measurements were carried out at room temperature at the XOR 3-ID HERIX beam line of the Advanced Photon Source, Argonne National Laboratory [23–25]. The synchrotron-based IXS technique provides meV energy resolution. It is a photon-in/photon-out spectroscopy where one measures both the energy and momentum changes of the scattered photon. The spectra were characterized by an elastic peak centered at zero energy and two inelastic peaks associated with the creation and annihilation of a phonon as shown in figure 3. We applied damped harmonic oscillator (DHO) model to describe the inelastic line shapes. The measured energy spectra were fitted with a model function convoluted with a pseudo-Voigt function for the instrument resolution which was measured separately. The model function consists of a Lorentzian distribution for the elastic part and a pair of Lorentzians, constrained by the thermal phonon population factor, for the inelastic part. The measurements were performed with a momentum resolution of 0.7 nm^{-1} by a slit in front of the analyzer. The distribution of this momentum resolution would introduce a distribution in the excitation energy and the measured phonon linewidth would be affected by this energy distribution. We therefore subtracted the phonon linewidth due to the limited momentum resolution and obtained the phonon linewidth due to phonon–phonon scattering. After fitting each q point, we obtained the phonon dispersion and linewidths. The inverse of phonon linewidths give phonon lifetimes.

The measured phonon frequency versus wavevector along three high symmetry lines are plotted in figure 4 along with the calculated dispersions. The detailed calculation procedure can be found elsewhere [9, 15, 17]. The accuracy of the DFPT force constants incorporated into the VC model has been borne out by the detailed study in PbSe and PbTe [9]. In general, our

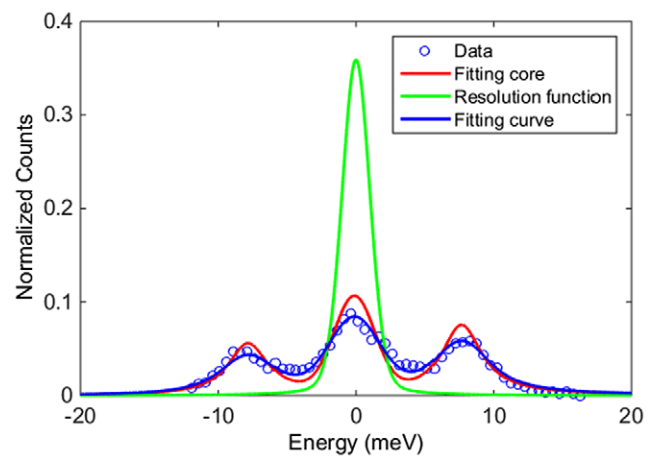


Figure 3. Typical energy spectra from the measurement (in blue circles), resolution function in green and the model function in red. The blue solid line denoted the convolution between the resolution function and the fitting core.

experimental results agree satisfactorily with those of the VC calculations. Even the Kohn-like anomaly around the zone center along [100] TA and [110] TA are matched to certain extent. The good agreement indicates that the VC model is a reasonable approximation in predicting the acoustic phonon dispersion of the $\text{PbTe}_{1-x}\text{Se}_x$ alloys. Considering that the phonon dispersion of pure PbSe and pure PbTe, as shown in figure 4(c), are not far apart from each other, the average quantities utilized by the VC model tend to be a good estimation for their alloys. This good agreement also suggests that it is reasonable to estimate phonon group velocities using the VC model, which has also been pointed out by Larkin and McGaughey [14].

Notably, one exception is the [111] TA modes. While the calculated dispersion curves of [111] TAs for pure PbSe and PbTe surprisingly fall on top of each other (figure 4(c)), their averaged properties overestimate [111] TA modes for $\text{PbTe}_{0.5}\text{Se}_{0.5}$ (figure 4(b)). In other words, the softening of [111] TA modes are intriguing, but not captured by simply averaging the quantities in the VC model. The ability to capture the softening is essential for the accurate prediction of thermal conductivity because the softening not only

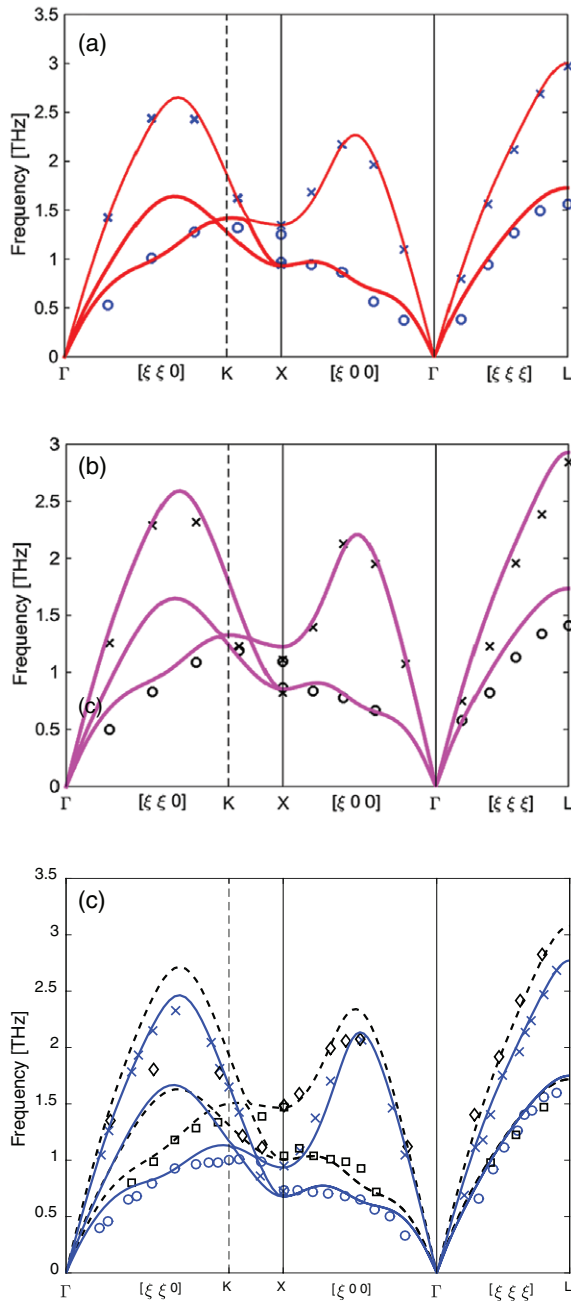


Figure 4. Markers are measured acoustic phonon dispersion: circles for transverse acoustic (TA) modes and crosses for longitudinal acoustic (LA) modes; solid lines are calculated acoustic phonon dispersion based on virtual crystal model for (a) $\text{PbTe}_{0.25}\text{Se}_{0.75}$ (b) $\text{PbTe}_{0.5}\text{Se}_{0.5}$. (c) Calculated phonon dispersion based on DFPT (lines: blue solid line for PbTe and black dashed line for PbSe) based on our earlier work [9] and measured phonon dispersion by inelastic neutron scattering (markers) from [29, 30] for PbSe and PbTe: blue circles for PbTe TA modes and blue crosses for PbTe LA modes; black squares for PbSe TA modes and black diamonds for PbSe LA modes. The error bars are smaller than the size of the circles/crosses in the figure.

influences the frequencies of these modes but affects phonon-phonon scattering rates as well. The softening can be related to the transition from independent scatterers in the dilute limit to the dependent scattering in the highest concentration limit. The softening may also relate to the slight distortion from

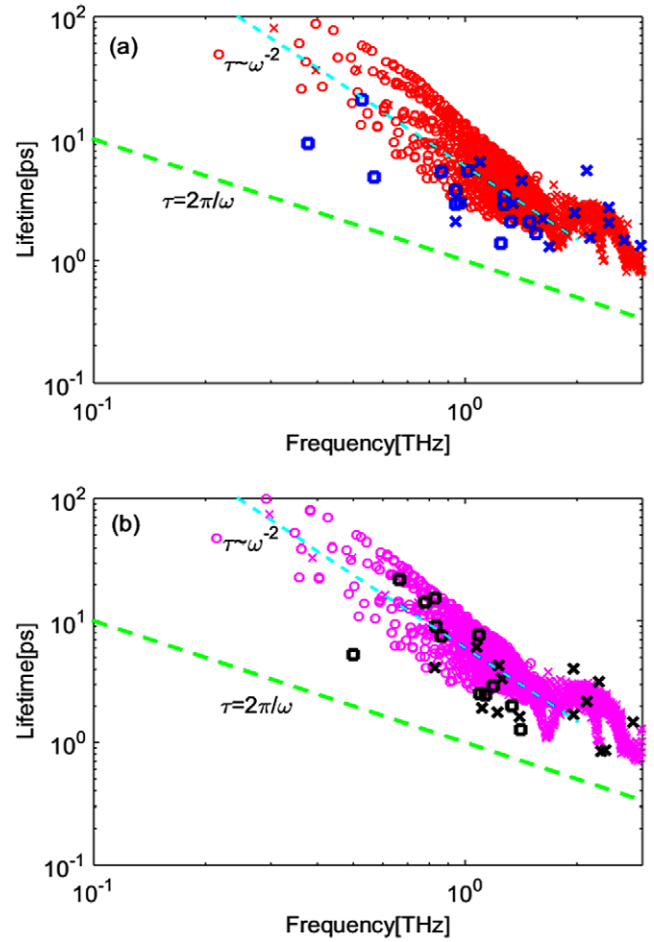


Figure 5. Measured acoustic phonon lifetimes and calculated acoustic phonon lifetimes based on virtual crystal model as a function of phonon frequencies: circles for transverse acoustic (TA) modes and crosses for longitudinal acoustic (LA) modes for (a) $\text{PbTe}_{0.25}\text{Se}_{0.75}$ (red: calculated and blue: measured) and (b) $\text{PbTe}_{0.5}\text{Se}_{0.5}$ (mauve: calculated and black: measured). Green dashed line denotes the Ioffe–Regel limit. The error bars are smaller than the size of the circles/crosses in the figure.

the perfect crystalline structure suggested by XRD. Phonon softening was observed in metal alloys and was attributed to structural phase transition [26–28], yet there is no experimental evidence of phase transition in $\text{PbTe}_{1-x}\text{Se}_x$ alloys. A deep understanding of the [1 1 1] TA modes in $\text{PbTe}_{1-x}\text{Se}_x$ alloys requires future investigation.

While the direct comparison of dispersion curves between the experiments and calculations gives us confidence in the phonon frequencies and group velocities based on the VC model, the discrepancy of thermal conductivity between the calculations and experiments as shown in figure 1 has to be attributed to phonon lifetimes. We plot the measured phonon lifetimes against the calculated phonon lifetimes in figure 5. It shows that the VC model in general moderately overestimates phonon lifetimes for both samples. This may due to the following facts: (1) The calculated lifetimes did not include the influence from the difference in bonding strengths and lengths. While the mass ratio between Ge and Si is 2.6 and mass-disorder dominates the disorder scattering, the mass difference between PbSe and PbTe is only 17% and the force

constant difference could be more profound. The inclusion of bond strength difference has been found to be important for $\text{PbTe}_{1-x}\text{Se}_x$ alloys [31–33]. The current overestimation in lifetimes reiterates the importance of bond disorder in phonon-disorder scattering. (2) Higher-order terms were neglected while treating the point-defect scattering in the calculation. The impurity scattering rates from first-order perturbation can deviate from the full perturbation solutions especially for the non-dilute regime [19, 33]. Whether the perturbation theory should hold in the non-dilute limit is another question. (3) The samples were considered as perfect crystals and defect scattering in real samples was not included in the calculation. Our experimental data on phonon lifetimes provide a benchmark for future refined theoretical endeavors to directly compare lifetimes and advance our understanding of the thermal transport in alloys. Meanwhile, it is noted that the frequency dependence trends of lifetimes are about the same for the VC model and IXS measurements, following a ω^{-2} dependence in the low frequency regime as predicted by Klemens [34].

Based on figure 5, all the modes are above the Ioffe–Regel limit of $\tau = 2\pi/\omega$, indicating phonons remain a good representation of the vibrational modes in $\text{PbTe}_{1-x}\text{Se}_x$ alloys. This is similar to earlier experiments on $\text{Ni}_{55}\text{Pd}_{45}$ alloys with substantial mass disorder using inelastic neutron scattering [35].

In summary, we have measured phonon transport properties in $\text{PbTe}_{1-x}\text{Se}_x$ alloys using IXS and compared with our calculations based on the VC model. Our experiments provide a critical test for validity of the VC model. In general, the VC model is a good approximation for phonon dispersions, i.e. phonon frequencies and group velocities in $\text{PbTe}_{1-x}\text{Se}_x$. Special attention, however, is drawn to the softening of TA [111] modes in the highest concentration limit. A thorough investigation of the softening may unveil details about the underlying transition picture. The VC model including only mass disorder, however, overestimates the phonon lifetimes for $\text{PbTe}_{1-x}\text{Se}_x$ alloys where bond disorder becomes important. More importantly, future theoretical efforts to include the dependent scattering are desirable. Our experimental data for phonon lifetimes can serve as a reference for future refined theoretical treatment of $\text{PbTe}_{1-x}\text{Se}_x$ alloys, and we also conclude that it is reasonable to describe the vibrational modes in this material as phonons. Our study paves the way for a deeper understanding of phonon transport in alloy systems and may help the design of alloys for thermoelectric conversion and other applications.

Acknowledgments

Z T acknowledges valuable discussion with Professor Gang Chen and Jonathan Mendoza at MIT. Z T is also grateful to Professor Nenad Miljkovic at UIUC for his help with focused ion beam. This material was supported by the S3TEC, an Energy Frontier Research Center funded by the US Department of Energy, Office of Science, Office of Basic Energy Sciences under Award Number DE-FG02-09ER46577. Use of the Advanced Photon Source, an Office of Science User Facility operated for the US Department of Energy (DOE) Office of Science by Argonne National Laboratory, was supported by the US DOE under Contract No. DE-AC02-06CH11357.

References

- [1] Goldsmid H J 2010 *Springer Ser. Mater. Sci.* **121** 1
- [2] Snyder G J and Toberer E S 2008 *Nat. Mater.* **7** 105
- [3] Sootsman J R, Chung D Y and Kanatzidis M G 2009 *Angew. Chem. Int. Ed.* **48** 8616
- [4] Zebarjadi M, Esfarjani K, Dresselhaus M S, Ren Z F and Chen G 2012 *Energy Environ. Sci.* **5** 5147
- [5] Tian Z T, Lee S and Chen G 2013 *J. Heat Transfer* **135** 061605
- [6] Tritt T M and Subramanian M A 2006 *MRS Bull.* **31** 188
- [7] Minnich A J, Dresselhaus M S, Ren Z F and Chen G 2009 *Energy Environ. Sci.* **2** 466
- [8] Pei Y Z, Shi X Y, LaLonde A, Wang H, Chen L D and Snyder G J 2011 *Nature* **473** 66
- [9] Tian Z T, Garg J, Esfarjani K, Shiga T, Shiomi J and Chen G 2012 *Phys. Rev. B* **85** 184303
- [10] Zhang Q, Cao F, Liu W S, Lukas K, Yu B, Chen S, Opeil C, Broido D, Chen G and Ren Z F 2012 *J. Am. Chem. Soc.* **134** 10031
- [11] Klemens P G 1958 *Solid State Phys. Adv. Res. Appl.* **7** 1
- [12] Allen P B, Feldman J L, Fabian J and Wooten F 1999 *Phil. Mag. B* **79** 1715
- [13] Beltukov Y M, Kozub V I and Parshin D A 2013 *Phys. Rev. B* **87** 134203
- [14] Larkin J M and McGaughey A J H 2013 *J. Appl. Phys.* **114** 023507
- [15] Abeles B 1963 *Phys. Rev.* **131** 1906
- [16] Tamura S 1983 *Phys. Rev. B* **27** 858
- [17] Garg J, Bonini N, Kozinsky B and Marzari N 2011 *Phys. Rev. Lett.* **106** 045901
- [18] Pettes M T, Sadeghi M M, Ji H, Jo I, Wu W, Ruoff R S and Shi L 2015 *Phys. Rev. B* **91** 035429
- [19] Mendoza J, Esfarjani K and Chen G 2015 *J. Appl. Phys.* **117** 174301
- [20] Ioffe A V and Ioffe A F 1960 *Sov. Phys.-Solid State* **2** 719
- [21] Chen G 2005 *Nanoscale Energy Transport and Conversion: a Parallel Treatment of Electrons, Molecules, Phonons, and Photons* (New York: Oxford University Press) p184
- [22] Matsushita Y, Wiannecki P A, Sommer A T, Geballe T H and Fisher I R 2006 *Phys. Rev. B* **74** 134512
- [23] Sinn H *et al* 2001 *Nucl. Instrum. Methods Phys. Res. A* **467** 1545
- [24] Toellner T S, Alatas A and Said A H 2011 *J. Synchrotron Radiat.* **18** (Pt 4) 605
- [25] Alatas A, Leu B M, Zhao J, Yavaş H, Toellner T S and Alp E E 2011 *Nucl. Instrum. Methods Phys. Res. A* **649** 166
- [26] Wong J, Krisch M, Farber D L, Occelli F, Schwartz A J, Chiang T C, Wall M, Boro C and Xu R Q 2003 *Science* **301** 1078
- [27] Ener S, Mehaddene T, Pedersen B, Leitner M, Neuhaus J and Petry W 2013 *N. J. Phys.* **15** 123016
- [28] Ohba T, Kitanosono D, Morito S, Fukuda T, Kakeshita T, Baron A Q R and Tsutsui S 2008 *Mater. Sci. Eng. A* **481** 254
- [29] Vijaraghavan P R, Sinha S K and Iyengar P K 1973 *Proc. Nuclear Physics and Solid State Symp.* vol **16**
- [30] Cochran W, Cowley R A, Dolling G and Elcombe M M 1966 *Proc. R. Soc. Lond. A* **293** 8
- [31] Murakami T, Shiga T, Hori T, Esfarjani K and Shiomi J 2013 *Epl* **102** 46002
- [32] Koh Y K, Vineis C J, Calawa S D, Walsh M P and Cahill D G 2009 *Appl. Phys. Lett.* **94** 153101
- [33] Katcho N A, Carrete J, Li W and Mingo N 2014 *Phys. Rev. B* **90** 094117
- [34] Klemens P G 1951 *Proc. R. Soc. Lond. A-Math. Phys. Sci.* **208** 108
- [35] Kamitaka W A and Brockhou B N 1974 *Phys. Rev. B* **10** 1200